Exhibit C

J. Med. Chem. 2004, 47, 4054−4059

Discovery of the Pyrrolo[2,1-*f*][1,2,4]triazine Nucleus as a New Kinase Inhibitor Template

John T. Hunt,*,§ Toomas Mitt,§,‡ Robert Borzilleri,§ Johnni Gullo-Brown,† Joseph Fargnoli,† Brian Fink,§ Wen-Ching Han,§ Steven Mortillo,† Gregory Vite,§ Barri Wautlet,† Tai Wong,† Chiang Yu,† Xiaoping Zheng,§ and Rajeev Bhide§

Departments of Oncology Chemistry, and Oncology Drug Discovery, Bristol-Myers Squibb Pharmaceutical Research Institute, P. O. Box 4000, Princeton, New Jersey 08543-4000

Received February 4, 2004

The pyrrolo[2,1-*f*][1,2,4]triazine nucleus was identified as a novel kinase inhibitor template which effectively mimics the well-known quinazoline kinase inhibitor scaffold. Attachment of a 4-((3-chloro-4-fluorophenyl)amino) substituent to the template provided potent biochemical inhibitors of the tyrosine kinase activity of EGFR, as well as inhibition of cellular proliferation of the human colon tumor cell line DiFi. Attachment of a 4-((3-hydroxy-4-methylphenyl)amino) substituent provided potent inhibitors of VEGFR-2 which also showed effects on the VEGF-dependent proliferation of human umbilical vein endothelial cells. Biological activity was maintained with substitution at positions 5 or 6, but not 7, suggesting that the former positions are promising sites for introducing side chains which modulate physicochemical properties. Preliminary inhibition studies with varying ATP concentrations suggest that, like the quinazoline-based kinase inhibitors, the pyrrolotriazine-based inhibitors bind in the ATP pocket.

Introduction

In the past decade, efforts aimed at the discovery of therapeutically useful inhibitors of protein kinases have intensified. These efforts have resulted in the identification of a variety of templates which, depending upon the nature of attached substituents, provide selective inhibition both within and across different protein kinase families.[1,2] One of these privileged scaffolds is the quinazoline nucleus **1** (Figure 1), which has served as the core template for a variety of ATP-competitive kinase inhibitors.[3] The leading examples of reversible quinazoline-based inhibitors are the clinically approved anticancer agent Iressa (**1a**, ZD1839) and OSI 774/CP 358,774 (**1b**, Tarceva), which is in Phase III clinical trials for cancer.[4,5] Both compounds are inhibitors of the receptor tyrosine kinase (RTK) activity of the epidermal growth factor receptor (EGFR/HER1), with relative selectivity for EGFR inhibition provided by the substituted aniline at position 4 and substituted alkoxy groups at positions 6 and 7. Two quinazoline-based drug candidates, one reversible (GW-572016/GW2016) and one irreversible (CI1033), which target both EGFR and the related RTK HER2 have been advanced into clinical trials.[6,7] Outside of the HER family, clinical compounds based on the quinazoline scaffold which target vascular endothelial growth factor receptor-2 (VEGFR-2/KDR) have been advanced into clinical trials.[8] Additionally, there are reports of other quinazoline-based RTK inhibitors, including compounds which target the tyrosine kinase activity of the platelet-derived growth factor receptor (PDGFR).[9]

With respect to the structure−activity relationships for kinase inhibition by quinazolines, the nitrogen at position 3 is important to EGFR inhibitory potency, but the nitrogen at position 1 is an even more important contributor.[10] Electron-donating substituents on the quinazoline ring improve potency, as do specifically substituted C4-anilines. For VEGFR-2 inhibition, the key pharmacophores of the quinazoline inhibitors are reported to be N-1 and specifically substituted C4-anilines.[11]

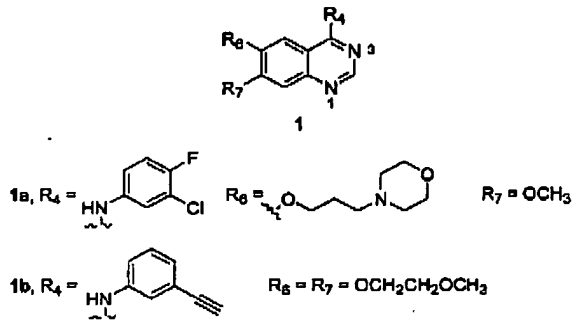

Figure 1. Structures of Iressa (**1a**) and Tarceva (**1b**), quinazoline-based inhibitors of the tyrosine kinase activity of EGFR.

The search for novel analogues of the quinazoline template has generated kinase inhibitors containing a variety of carbon-fused heterocycles, where the potential for maintaining key pharmacophores is intact.[1] For example, the effects on EGFR inhibition of replacing the fused benzene of the quinazoline ring system with each of the isomeric pyridines has been studied.[12] Because of the substantial prior art with 6,6-fused analogues of quinazolines, we were intrigued by the possibility that insertion of a nitrogen at a ring-fusion position could generate novel quinazoline mimics. In addition, the aza-fusion would mandate a 5,6-ring system. It has been generally found that substitution at positions 6 and 7 on the fused benzene ring of quinazoline-based kinase inhibitors is well tolerated, and these positions are often

* To whom correspondence should be addressed. Tel: (609) 252-4989. Fax: (609) 252-6171. E-mail: John.hunt@bms.com.
§ Department of Oncology Chemistry.
† Department of Oncology Drug Discovery.
‡ Deceased March 7, 2004.

10.1021/jm049892u CCC: $27.50
Published on Web 06/23/2004

Scheme 1. Synthesis of Pyrrolotriazine Kinase Inhibitors[a]

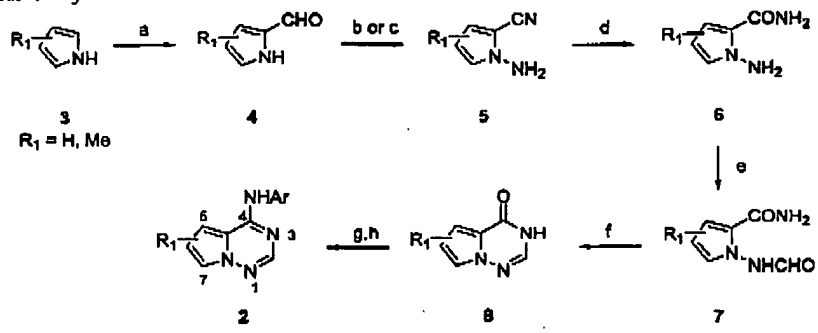

[a] (a) DMF, $POCl_3$, 1,2-dichloroethane; (b) hydroxylamine-*O*-sulfonic acid, KOH, water; (c) *O*-mesitylenesulfonylhydroxylamine, NaH, CH_2Cl_2; (d) KOH; (e) HCO_2H, NaOAc; (f) NaOMe, MeOH; (g) $POBr_3$; (h) 3-chloro-4-fluoro-phenylamine or 5-amino-2-methylphenol, acetonitrile.

utilized to vary physical and pharmacokinetic properties of drug candidates. Replacement of the carbon-fused ring with a nitrogen-fused ring would allow the fused six-member ring to be replaced with a five-member ring, allowing attachment of side chains to 3 positions, each of which projects into space with a different geometry than quinazoline 6- or 7-substituents.

In this report, we describe our initial progress on aza-fused kinase inhibitors based on the quinazoline nucleus. In particular, we describe preliminary synthetic and structure–activity relationships of pyrrolo[2,1-*f*][1,2,4]-triazine inhibitors **2** of VEGFR-2 and EGFR.

Chemistry. The initial pyrrolotriazine targets were prepared according to a reported procedure (Scheme 1) through the intermediacy of the requisite pyrrolotriazinones **8**.[13] The methyl-substituted 2-formylpyrroles **4** were prepared from the pyrroles **3** by reaction with phosphorus oxychloride and DMF in yields ranging from 18 to 89%. An isomeric mixture of 2-formyl-3-methylpyrrole and 2-formyl-4-methylpyrrole in a 4:1 ratio was produced from the formylation of 3-methylpyrrole. Amination of this mixture with hydroxylamine *O*-sulfonic acid produced both N-amination as well as transformation of the aldehyde to the nitrile to form **5** (isomeric mixture of R_1 = 3-methyl and 4-methyl) in 20% overall yield. The same set of transformations produced **5** (R_1 = 5-methyl) in 65% yield by treatment of 5-methyl-2-formylpyrrole with *O*-mesitylenesulfonylhydroxylamine (MSH) in DMF followed by NaH. For 2-formyl-3,4-dimethylpyrrole, transformation to **5** (R_1 = 3,4-dimethyl) was produced by a two-step reaction sequence involving treatment with aqueous hydroxylamine *O*-sulfonic acid (37% yield) and subsequent N-amination by treatment with MSH followed by NaH (94% yield). Hydrolysis of the isomeric mixture of 1-amino-2-cyano-3-methylpyrrole and 1-amino-2-cyano-4-methylpyrrole with aqueous KOH at room temperature produced 1-amino-2-aminocarbonyl-4-methylpyrrole (**6**, R_1 = 4-methyl, 61% yield), leaving the 1-amino-2-cyano-3-methylpyrrole unreacted and separable. The 1-amino-2-cyano-5-methylpyrrole was similarly hydrolyzed to **6** (R_1 = 5-methyl) in 94% yield. Hydrolysis of the pure 1-amino-2-cyano-3-methylpyrrole was achieved with KOH in aqueous ethanol at reflux to form **6** (R_1 = 3-methyl) in 82% yield. Formylation of the 1-amino group to form **7** in yields ranging from 76 to 89% was achieved with formic acid and sodium acetate. In the case of the dimethyl isomer **6** (R_1 = 3,4-dimethyl), heating at 65 °C in a mixture of formic acid and sodium acetate led directly to the cyclized product **8** (R_1 = 5,6-dimethyl). For the remaining compounds, cyclization was achieved with sodium methoxide in methanol in 53–80% yields. Activation of the 4-position was generally achieved with phosphorus oxybromide, and reaction with the requisite anilines in acetonitrile provided the target compounds in two step yields ranging from 19 to 49%. In the case of compound **10**, activation was achieved with phosphorus oxychloride, and the two-step yield was 85%.

Biological Testing. Kinase inhibition assays were performed in standard fashion, using the entire cytoplasmic sequences of EGFR and VEGFR-2 fused to glutathione S-transferase (GST-HER1, GST-VEGFR-2). Activity was determined by quantitation of the amount of radioactive phosphate transferred to the poly(Glu_4/Tyr) substrate. Enzyme assays to shed light on the ATP-competitive nature of the inhibitors were performed at ATP concentrations of 1 and 10 μM. Cellular assays for EGFR activity measured the ability of compounds to inhibit proliferation of DiFi human colon tumor cells or to inhibit proliferation of human umbilical vein endothelial cells (HUVECs) driven by EGF. Cellular assays for VEGFR-2 activity measured the ability of compounds to inhibit proliferation of HUVECs driven by the mitogen VEGF.

Structure–Activity Relationships. To ascertain whether the pyrrolo[1,2,4]triazine nucleus was capable of affording potent kinase inhibitors, we focused on two kinases for which a variety of potent quinazoline inhibitors are known, namely EGFR and VEGFR-2. For these studies, we selected key C4-anilino side chains which have been shown in analogous quinazoline inhibitors to provide potent inhibition of the kinase activity of these RTKs. These side chains were the 4-(3-chloro-4-fluorophenyl)amino group, present in the clinical EGFR inhibitor Iressa, and the 4-(3-hydroxy-4-methylphenyl)-amino group, a representative side chain present in a potent preclinical series of VEGFR-2 inhibitors.[4,11] The initial analogues prepared contained an otherwise unsubstituted pyrrolo[1,2,4]triazine, as well as substitution patterns with a single methyl group at either the 5-, 6-, or 7-positions.

Attachment of the (3-chloro-4-fluorophenyl)amino Iressa side chain to the 4-position of the unsubstituted

Table 1. Enzymatic and Cellular Activity of Pyrrolotriazine Kinase Inhibitors

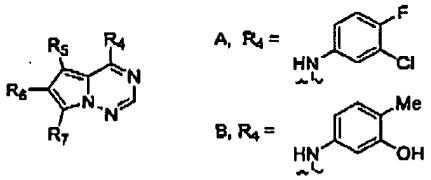

					biochemical IC_{50} (μM)		cellular IC_{50} (nM)	
compd	R_4	R_5	R_6	R_7	VEGFR-2	EGFR	HUVEC: VEGF/EGF	DiFi
9	A	H	H	H	>10	0.118	>2500/345	1840
10	A	Me	H	H	>10	0.100	>2500/602	3060
11	A	H	Me	H	>2	0.151	>2500/509	1600
12	A	H	H	Me	>2	3.25	>2500/>2500	>10000
13	B	H	H	H	1.44 ± 0.95	0.51	360/ND[a]	>10000
14	B	Me	H	H	0.066	0.346	98 ± 88/270	>10000
15	B	H	Me	H	0.405	0.654	213 ± 89/644	>10000
16	B	H	H	Me	>10	29.4	477 ± 92/101	>10000
17	B	Me	Me	H	0.023	0.200	310/ND	>10000

[a] ND = not determined.

pyrrolo[1,2,4]triazine nucleus afforded compound **9**, which was a relatively potent inhibitor (IC_{50} = 118 nM) of the tyrosine kinase activity of EGFR (Table 1). For an initial analogue, this potency compares favorably to the reported IC_{50} value for Iressa (23 nM).[4] Appendage of a methyl group to either the 5- or 6-position of the pyrrolotriazine provided analogues **10** and **11**, respectively, which showed inhibitory potency similar to the unsubstituted compound **9**. The 7-methyl analogue **12** was substantially poorer as an inhibitor of EGFR, suggesting that this RTK makes close contacts with the pyrrolo[1,2,4]triazine nucleus in the region around the 7-position. Keeping in mind the slightly different vectors produced by the 7-pyrrolotriazine and 8-quinazoline substituents, these data are consistent with the observation that 8-substituents in the quinazoline-based EGFR inhibitors do not generally lead to improved biochemical potency.[10]

Attachment of the (3-hydroxy-4-methylphenyl)amino substituent to the 4-position of the unsubstituted nucleus afforded compound **13** which was a moderately potent inhibitor of the tyrosine kinase activity of both VEGFR-2 and EGFR. Incorporation of a 5-methyl group provided analogue **14** which showed slightly increased inhibition of EGFR but substantially increased inhibition of VEGFR-2. The 6-methyl analogue **15** was intermediate at inhibiting VEGFR-2 and roughly equivalent to the parent **13** against EGFR. Again, the 7-methyl analogue **16** was dramatically poorer as an inhibitor of both EGFR and VEGFR-2, indicating that each of these RTKs has steric requirements which are quite stringent in this area of the inhibitor. Interestingly, the 5,6-dimethyl analogue **17** was the most potent inhibitor identified of the tyrosine kinase activity of VEGFR-2, with an IC_{50} value of 23 nM. Improvements in potency with the modestly electron-donating methyl groups in this series parallel findings that the strongly electron-donating 6- and 7-alkoxy groups provide increased inhibitory potency in the quinazoline-based EGFR inhibitors.[10]

To gain some insight into the kinetic mechanism of enzyme inhibition by this new class of inhibitors, IC_{50} values against EGFR were determined for a selected compound in the presence of different concentrations of ATP. The IC_{50} value for **9** against EGFR increased from 0.118 ± 0.013 μM to 1.11 ± 0.23 μM when the ATP concentration in the assay was raised from 1 μM to 10 μM. While far from conclusive, these preliminary data support the presumption that the pyrrolotriazine-based inhibitors are likely to be ATP competitive, a finding which would not be surprising, considering the fact that the quinazoline-based inhibitors from which the corresponding pyrrolotriazine inhibitors were derived are known to be ATP-competitive inhibitors.[14,11,15]

Cellular assays were undertaken to explore whether this new inhibitor class was capable of providing inhibitors of the cellular functions of the EGFR and VEGFR-2 receptors. Compounds were tested for their ability to inhibit the proliferation of the human colon adenocarcinoma cell line DiFi, which overexpresses EGFR and is known to be sensitive to EGFR inhibitors. Compounds were also tested for their ability to inhibit the proliferation of human umbilical vein endothelial cells (HUVECs) driven by either of the mitogens EGF or VEGF. In the DiFi tumor cell line, each of the submicromolar inhibitors of EGFR (**9**, **10**, **11**) demonstrated inhibition of cellular proliferation in the low micromolar range, while the cellular IC_{50} value was greater than 10 μM for the less potent EGFR biochemical inhibitor **12**. In accord with their biochemical potencies, none of the EGFR selective compounds **9**, **10**, **11** or **12** inhibited the proliferation of HUVECs driven by VEGF. Again in accord with their biochemical potencies, the submicromolar EGFR inhibitors **9**, **10** and **11** inhibited the proliferation of HUVECs driven by EGF with submicromolar potencies.

The cellular behavior of the compounds with the phenol side chain, which were biochemical inhibitors of both VEGFR-2 and EGFR, was less easily interpretable. Several analogues (**13**, **14**, **15**, **17**) which displayed submicromolar IC_{50} values for EGFR inhibition inhibited HUVEC proliferation driven by EGF, but these compounds did not inhibit the cellular proliferation of DiFi cells. Unexpectedly, all of the compounds with the phenolic side chain (**13**–**17**) were moderate to potent inhibitors of HUVEC proliferation, regardless of the mitogen employed or the potency of the analogue against VEGFR-2 or EGFR. For example, the inhibition of HUVEC proliferation by **14** is not unexpected,

considering that it is a submicromolar inhibitor of both VEGFR-2 and EGFR. On the contrary, the inhibition of VEGF- or EGF-driven HUVEC proliferation by **16** is completely unexpected, considering that it is a very poor inhibitor of both VEGFR-2 and EGFR. At the present time, we have no explanation for the behavior in the HUVEC proliferation assay of the pyrrolotriazines containing the phenolic side chain. Despite some inconsistencies in the cellular behavior of the phenol derivatives, both chemical series demonstrated sufficient cellular activity to showcase the potential value of RTK inhibitors derived from the pyrrolo[1,2,4]triazine nucleus.

Conclusions

A search for novel kinase inhibitor templates identified the pyrrolo[1,2,4]triazine nucleus as one which effectively mimics the well-known quinazoline kinase inhibitor template. Attachment of C4-substituents which were known from quinazoline-based compounds to confer inhibitory activity against the kinase activity of EGFR or VEGFR-2 provided potent pyrrolotriazine-based inhibitors of these receptor tyrosine kinases. Initial structure–activity studies identified positions 5 and 6 as ones which tolerated substitution, while substitution at the 7-position led to substantial loss of inhibitory activity. Confirming the importance of this new class of kinase inhibitors, many of the compounds were also shown to have substantial activity in cellular assays. Future reports will detail the application of the pyrrolo[1,2,4]triazine nucleus to the design of potent and selective inhibitors of a variety of kinases, and the demonstration of inhibitor efficacy in preclinical disease models.

Experimental Section

In Vitro Kinase Assays. Recombinant proteins that consisted of the entire cytoplasmic sequences of HER1 (GST-HER1) and VEGFR-2 (GST-VEGFR-2) fused to glutathione S-transferase were prepared by expression in Sf9 insect cells of the fusion cDNA. The protein was isolated by affinity chromatography using glutathione-Sepharose. Kinase assays were performed in 96-well microtiter plates using the synthetic polymer poly(Glu$_4$/Tyr) (Sigma Chemicals) as a phosphoacceptor substrate. Test compounds were dissolved in DMSO and diluted with water/1% DMSO. Final concentration of DMSO in assay solutions was 0.5%, which was shown to have no effect on kinase activity. Assay conditions were (VEGFR-2; HER1): total volume (50 μL; 50 μL), enzyme (7.5 ng; 10 ng), substrate (75 μg/mL; 100 μg/mL), ATP (2.5 μM and 0.04 μCi of [γ-^{33}P]-ATP; 1 μM and 0.15 μCi of [γ-^{33}P]ATP), kinase buffer (20 mM Tris, pH 7.0, 0.5 mM DTT, 25 μg/mL BSA, 1.5 mM MnCl2; 50 mM Tris, pH 7.5, 0.5 mM DTT, 0.1 mg/mL BSA, 10 mM MnCl2), reaction conditions (27 °C, 1 h; 28 °C, 1 h), assay quench (50 μL of 30% trichloroacetic acid on ice; 10 μL of buffer consisting of 2.5 mg/mL BSA and 300 mM EDTA, followed by immediate precipitation with 110 μL of 10% TCA on ice for 30 min). The precipitates were transferred to 96-well UniFilter GF/C plates (Packard Instrument Co.) using a Filtermate universal harvester. The amount of phosphorylated substrate was quantitated using a TopCount 96-well liquid scintillation counter (PerkinElmer Life Sciences). Dose–response curves were generated to determine the concentration of inhibitor required to inhibit 50% of kinase activity (IC_{50}). For VEGFR-2, compounds were dissolved in dimethyl sulfoxide (DMSO) to a concentration of 10 mM and were evaluated at six concentrations diluted 4-fold, each in triplicate. For HER1, compounds were dissolved in 100% DMSO and diluted into 2× the final concentration with water/1% DMSO prior to assay.

Cell Based Assays. HUVEC Proliferation Assay. Primary human umbilical vein endothelial cells (HUVECs) were purchased from Clonetics and not used beyond Passage 3 for mitogen-stimulated proliferation assays. For compound assessment, cells were plated in 100 μL minimal growth medium (Cellgro) and 1.0% fetal bovine serum, heat-inactivated in 96-well collagen IV-coated plates (Becton-Dickinson) at a density of 2 × 10^3 per well in a 37 °C/5% CO_2 environment. After 24 h, growth factor and test compound at various dilutions were added to each well in a final volume of minimal growth media that contained either VEGF (Peprotech) at 80 ng/mL, EGF (Clonetics) at 5 ng/mL, or no growth factors. After 48 h, 0.5 μCi of ^{3}H-thymidine (Amersham) was added in a volume of 20 μL minimal media, and the cells were incubated for 24 h. Plates were washed once in PBS. Upon removal of PBS, trypsin (Cellgro) was added to cells which were subsequently harvested onto glass fiber filters (Perkin-Elmer Life Sciences) using an automated harvester (Brandel Model# MWX RI-192TI). Incorporated tritium was quantified using a beta counter (Wallac Microbeta). Dose–response curves were generated to determine the IC_{50}, which is defined as the concentration of drug required to inhibit 50% of tritium incorporation when compared to untreated mitogen-stimulated cells.

DiFi Cell Proliferation Assay. Inhibition of cell proliferation was assessed by the MTS assay using a CellTiter 96 Aqueous Non-Radioactive Proliferation Assay kit (Promega). Cells were inoculated into 96-well microtiter plates and incubated at 37 °C, 5% CO_2, 95% air, and 100% relative humidity for 24 h prior to addition of drug. At the time of drug addition, one plate of the cell line was processed using the above kit to represent a measurement of the cell population at the time of drug addition (A_{0h}). Following drug addition, the plates were incubated for an additional 72 h before processing to measure the cell population (A_{72h} and A_c represent cell populations at 72h in the presence and absence of drug, respectively). Each compound was tested at eight different concentrations in triplicate in addition to control sample without any additions. Growth inhibition of 50% (IC_{50}) is calculated from $[(A_{72h} - A_{0h})/(A_c - A_{0h})] \times 100 = 50$, which is the drug concentration resulting in a 50% reduction in the net increase in cell population (as measured by MTS staining) of control cells during the drug incubation. Analysis of the data was done in Excel using a four-parameter logistic equation to calculate an IC_{50} with data fitted using the Levenburg Marquardt algorithm.

General Chemical Procedures. Proton NMR (^{1}H NMR) and carbon NMR (^{13}C NMR) spectra were obtained on JEOL Eclipse 400 and 500 or Bruker Avance 400 MHz spectrometers and are reported relative to tetramethylsilane (TMS) reference. Low resolution mass spectra were obtained on a Finnigan SSQ 700 spectrometer; high-resolution mass spectra were obtained on a Micromass LCT spectrometer; LC/MS was performed on a ThermoFinnigan LCQ Advantage system (Micromass). Analytical and preparative HPLC were performed on YMC columns (A-302, S-5, 120A ODS, 4.6 × 150 mm; SH-345-15, S-15, 120A ODS, 20 × 500 mm; ODA S 5m 4.6 × 500 mM) with acetonitrile:water gradients containing 0.1% trifluoroacetic acid. Chromatography was performed under flash conditions using EM Science silica 0.040–0.063 mm particle size. THF was either distilled from Na/benzophenone or obtained from EM Science Drisolv bottles. Solutions were dried with magnesium sulfate unless otherwise noted.

2-Methyl-5-[(6-methylpyrrolo[2,1-*f*][1,2,4]triazin-4-yl)-amino]phenol (15). To 3.15 mL (41 mmol) of DMF at 0 °C under argon was added dropwise 3.81 mL (41 mmol) of phosphorus oxychloride. The cooling bath was removed and stirring was continued for 15 min. The solution was diluted with 9 mL of 1,2-dichloroethane and again cooled to 0 °C. A solution of 3.0 g (37 mmol) of 3-methylpyrrole in 9 mL of 1,2-dichloroethane was added dropwise. The mixture was heated to reflux for 15 min and cooled to 0 °C, and a solution of 16.2 g (203 mmol) of sodium acetate in 45 mL of water was added with vigorous stirring. The mixture was heated at reflux for 20 min and allowed to cool to room temperature. The aqueous

layer was separated and extracted twice with methylene chloride. The combined organic layers were washed with sat $NaHCO_3$ until neutral, and dried, and the solvent was removed to yield a dark oily solid which was purified by flash chromatography (10% EtOAc:hexane) to afford 3.6 g (89%) of a 4:1 mixture of 2-formyl-3-methylpyrrole and 2-formyl-4-methylpyrrole (isomers of **4**, R_1 = Me) as a pale yellow solid. The isomeric mixture was aminated as previously described to form a 2:1 mixture of 1-amino-2-cyano-3-methylpyrrole and 1-amino-2-cyano-4-methylpyrrole (isomers of **5**, R_1 = Me) in 50% yield.[13] The mixture of nitriles was hydrolyzed as described to form 1-amino-2-aminocarbonyl-4-methyl-pyrrole (**6**, R_1 = 4-Me) as well as unreacted 1-amino-2-cyano-3-methylpyrrole, which were separated by flash chromatography (10% EtOAc:hexane). The conversion of 1-amino-2-cyano-3-methylpyrrole to 1-amino-2-aminocarbonyl-3-methyl-pyrrole (**6**, R_1 = 3-Me) was accomplished by performing the hydrolysis in aqueous ethanol at reflux for 2 h. Conversion of 1-amino-2-aminocarbonyl-4-methyl-pyrrole to 6-methyl-pyrrolo[2,1-*f*][1,2,4]triazin-4(3*H*)-one (**8**, R_1 = 6-Me) in 71% overall yield was performed as described.[13] A mixture of 23 mg (0.15 mmol) of 6-methyl-pyrrolo[2,1-*f*][1,2,4]triazin-4(3*H*)-one and 0.1 g of phosphorus oxybromide was heated at 60 °C for 20 min under argon. A melt was initially obtained which solidified on continued heating. Ice was added to the solid with vigorous stirring. The mixture was extracted twice with ethyl acetate. The combined extracts were washed with sat $NaHCO_3$ and brine and dried, and the solvent was removed to afford 25 mg of crude 4-bromo-6-methyl-pyrrolo[2,1-*f*][1,2,4]triazine as a yellow solid. A solution of this material and 20 mg (0.165 mmol) of 3-hydroxy-4-methylaniline in 0.5 mL of acetonitrile was stirred overnight at room temperature under argon. The mixture was evaporated to dryness, and the residue was diluted with EtOAc. Sufficient sat $NaHCO_3$ was added to generate the free base. The organic layer was separated and washed with brine and dried and the solvent removed. The residual solid was subjected to flash chromatography (25% EtOAc:hexanes) to yield 11 mg (0.04 mmol, 29%) of **15** as a tan solid. ^{1}H NMR (400 MHz, DMSO-d_6) δ 9.56 (s, 1H), 9.38 (s, 1H), 7.91 (s, 1H), 7.55 (s, 1H), 7.39 (d, 1H, J = 1.3 Hz), 7.12 (dd, 1H, J = 1.8, 8.1 Hz), 7.02 (d, 1H, J = 8.1 Hz), 6.97 (s, 1H), 2.26 (s, 3H), 2.10 (s, 3H). HRMS for $C_{14}H_{13}N_4O$ (M − H), Calcd: 253.1090, Found: 253.1094.

4-(2-Chloro-4-fluorophenylamino)-pyrrolo[2,1-*f*][1,2,4]-triazine (9). ^{1}H NMR (400 MHz, $CDCl_3$) δ 8.04 (s, 1H), 7.91 (dd, 1H, J = 2.8, 6.6 Hz), 7.65 (s, 1H), 7.50 (ddd, 1H, J = 3.3, 7.1, 9.3 Hz), 7.16 (t, 1H, J = 8.8 Hz), 6.92 (br s, 1H), 6.73 (dd, 1H, J = 2.8, 4.4 Hz), 6.61 (d, 1H, J = 4.4 Hz). ^{13}C NMR (125 MHz, acetone-d_6) δ 154.2 (d, J = 244.2 Hz), 152.2, 146.6, 136.3, 123.2, 121.5 (d, J = 7.6 Hz), 119.9 (d, J = 20.4 Hz), 119.4, 116.6 (d, J = 22.9 Hz), 114.5, 111.2, 101.0. HRMS for $C_{12}H_9N_4FCl$ (M + H). Calcd: 263.0510, Found: 263.0500.

4-(2-Chloro-4-fluorophenylamino)-5-methyl-pyrrolo-[2,1-*f*][1,2,4]triazine (10). ^{1}H NMR (125 MHz, $CDCl_3$/CD_3OD) δ 7.70 (s, 2H), 7.42 (s, 1H), 7.36−7.34 (m, 1H), 7.29−7.06 (m, 1H), 6.43 (s, 1H), 2.53 (s, 3H). ^{13}C NMR (125 MHz, $CDCl_3$/CD_3OD) δ 156.3, 154.3, 152.8, 145.0, 133.6, 125.0, 122.6, 121.0, 118.6, 116.6, 116.4, 113.6, 113.3, 111.3, 13.3. HRMS for $C_{13}H_{11}N_4FCl$ (M + H), Calcd: 276.0578, Found: 276.0599.

4-(2-Chloro-4-fluorophenylamino)-6-methyl-pyrrolo-[2,1-*f*][1,2,4]triazine (11). ^{1}H NMR (400 MHz, $CDCl_3$) δ 8.00 (s, 1H), 7.91 (dd, 1H, J = 2.8, 6.6 Hz), 7.50 (m, 2H), 7.16 (t, 1H, J = 8.8 Hz), 6.76 (br s, 2H), 6.42 (s, 1H), 2.33 (s, 3H). ^{13}C NMR (125 MHz, acetone-d_6) δ 154.4 (d, J = 244.2 Hz), 151.4, 145.9, 136.4, 123.0, 122.4, 121.3 (d, J = 7.6 Hz), 119.8 (d, J = 20.4 Hz), 118.4, 116.5 (d, J = 22.9 Hz), 114.4, 101.3, 11.5. HRMS for $C_{13}H_{11}N_4FCl$ (M + H), Calcd: 277.0656, Found: 277.0657.

4-(2-Chloro-4-fluorophenylamino)-7-methyl-pyrrolo-[2,1-*f*][1,2,4]triazine (12). ^{1}H NMR (400 MHz, $CDCl_3$) δ 8.10 (s, 1H), 7.93 (dd, 1H, J = 2.5, 6.1 Hz), 7.50 (ddd, 1H, J = 3.1, 4.0, 7.1 Hz), 7.16 (t, 1H, J = 8.7 Hz), 6.84 (br s, 1H), 6.58 (d, 1H, J = 4.6 Hz), 6.53 (d, 1H, J = 4.1 Hz), 2.55 (s, 3H). ^{13}C NMR (125 MHz, $CDCl_3$) δ 154.9 (d, J = 246.7 Hz), 151.9, 146.4, 134.6, 128.4, 124.1, 121.6 (d, J = 5.1 Hz), 121.1 (d, J = 17.8 Hz), 116.5 (d, J = 20.4 Hz), 113.6, 110.8, 99.4, 10.8. HRMS for $C_{13}H_{11}N_4FCl$ (M + H). Calcd: 277.0659, Found: 277.0657.

2-Methyl-5-(pyrrolo[2,1-*f*][1,2,4]triazin-4-ylamino)phenol (13). ^{1}H NMR (400 MHz, CD_3OD) δ 7.83 (s, 1H), 7.57 (dd, 1H, J = 1.6, 2.3 Hz), 7.31 (d, 1H, J = 1.6 Hz), 7.06 (d, 1H, J = 8.06 Hz), 6.96 (m, 2H), 6.69 (dd, 1H, J = 2.6, 4.3 Hz), 2.18 (s, 3H). ^{13}C NMR (125 MHz, CD_3OD) δ 156.8, 154.2, 148.1, 138.1, 131.6, 122.7, 119.9, 116.1, 115.1, 111.9, 110.9, 102.5, 15.8. HRMS for $C_{13}H_{12}N_4O$, Calcd: 240.1011, Found: 240.1014.

2-Methyl-5-[(5-methylpyrrolo[2,1-*f*][1,2,4]triazin-4-yl)-amino]phenol (14). ^{1}H NMR (400 MHz, DMSO-d_6) δ 9.35 (s, 1H), 8.24 (s, 1H), 7.82 (s, 1H), 7.61 (d, 1H, J = 2.5 Hz), 7.24 (d, 1H, J = 2.0 Hz), 7.02 (d, 1H, J = 8.1 Hz), 6.96 (dd, 1H, J = 2.0, 8.1 Hz), 6.63 (d, 1H, J = 2.4 Hz), 2.60 (s, 3H), 2.10 (s, 3H). HRMS for $C_{14}H_{13}N_4O$ (M − H), Calcd: 253.1090, Found: 253.1084.

2-Methyl-5-[(7-methylpyrrolo[2,1-*f*][1,2,4]triazin-4-yl)-amino]phenol (16). ^{1}H NMR (400 MHz, DMSO-d_6) δ 9.53 (s, 1H), 9.36 (s, 1H), 8.00 (s, 1H), 7.43 (d, 1H, J = 1.9 Hz), 7.12 (dd, 1H, J = 1.9, 8.1 Hz), 7.10 (d, 1H, J = 4.3 Hz), 7.02 (d, 1H, J = 8.1 Hz), 6.53 (d, 1H, J = 4.3 Hz), 2.44 (s, 3H), 2.10 (s, 3H). HRMS for $C_{14}H_{13}N_4O$ (M − H), Calcd: 253.1090, Found: 253.1094.

5-[(5,6-Dimethylpyrrolo[2,1-*f*][1,2,4]triazin-4-yl)amino]-2-methylphenol (17). ^{1}H NMR ($CDCl_3$, 400 MHz) δ 7.74 (s, 1H), 7.34 (s, 1H), 7.06 (d, 1 H, J = 8 Hz), 6.96 (d, 1H, J = 2 Hz), 6.65 (dd, 1H, J = 2, 8 Hz), 2.48 (s, 3H), 2.17 (s, 3H), 2.05 (s, 3H). HRMS for $C_{15}H_{16}N_4O$, Calcd: 268.1324, Found: 268.1330.

Acknowledgment. This manuscript is dedicated to the memory of Toomas (Tom) Mitt, whose exceptional experimental skills allowed the discovery of this novel kinase inhibitor template. We also thank the Department of Discovery Analytical Sciences for the mass spectral data, and Veeraswamy Manne for technical assistance.

References

(1) Garcia-Echeverria, C.; Traxler, P.; Evans, D. B. ATP Site-Directed Competitive and Irreversible Inhibitors of Protein Kinases. *Med. Res. Rev.* **2000**, *20*, 28−57.
(2) Dumas, J. Protein Kinase Inhibitors: Emerging Pharmacophores 1997−2000. *Expert Opin. Ther. Pat.* **2001**, *11*, 405−429.
(3) Ward, W. H. J.; Cook, P. N.; Slater, A. M.; Davies, D. H.; Holdgate, G. A. et al. Epidermal Growth Factor Receptor Tyrosine Kinase: Investigation of Catalytic Mechanism, Structure-Based Searching and Discovery of a Potent Inhibitor. *Biochem. Pharmacol.* **1994**, *48*, 659−666.
(4) Barker, A. J.; Gibson, K. H.; Grundy, W.; Godfrey, A. A.; Barlow, J. J. et al. Studies Leading to the Identification of ZD1839 (Iressa™): An Orally Active, Selective Epidermal Growth Factor Receptor Tyrosine Kinase Inhibitor Targeted to the Treatment of Cancer. *Bioorg. Med. Chem.* **2001**, *11*, 1911−1914.
(5) Moyer, J. D.; Barbacci, E. G.; Iwata, K. K.; Arnold, L.; Boman, B. et al. Induction of Apoptosis and Cell Cycle Arrest by CP-358, 774, an Inhibitor of Epidermal Growth Factor Receptor Tyrosine Kinase. *Cancer Res.* **1997**, *57*, 4838−4848.
(6) Kim, T. E.; Murren, J. R. Lapatinib Ditosylate. *IDrugs* **2003**, *6*, 886−893.
(7) Smaill, J. B.; Rewcastle, G. W.; Loo, J. A.; Greis, K. D.; Chan, O. H. et al. Tyrosine Kinase Inhibitors. 17. Irreversible Inhibitors of the Epidermal Growth Factor Receptor: 4-(Phenylamino)-quinazoline- and 4-(Phenylamino)pyrido[3,2-*d*]pyrimidine-6-acrylamides Bearing Additional Solubilizing Functions. *J. Med. Chem.* **2000**, *43*, 1380−1397.
(8) Hennequin, L. F.; Stokes, E. S. E.; Thomas, A. P.; Johnstone, C.; Ple, P. A. et al. Novel 4-Anilinoquinazolines with C-7 Basic Side Chains: Design and Structure Activity Relationship of a Series of Potent, Orally Active, VEGF Receptor Tyrosine Kinase Inhibitors. *J. Med. Chem.* **2002**, *45*, 1300−1312.
(9) Matsuno, K.; Nakajima, T.; Ichimura, M.; Giese, N. A.; Yu, J.-C. et al. Potent and Selective Inhibitors of PDGF Receptor Phosphorylation. 2. Synthesis, Structure Activity Relationship, Improvement of Aqueous Solubility, and Biological Effects of 4-[4-(N-Substituted (thio)carbamoyl)-1-piperazinyl]-6,7-dimethoxyquinazoline Derivatives. *J. Med. Chem.* **2002**, *45*, 4513−4523.
(10) Rewcastle, G. W.; Denny, W. A.; Bridges, A. J.; Zhou, H.; Cody, D. R. et al. Tyrosine Kinase Inhibitors. 5. Synthesis and Structure−Activity Relationships for 4-[(Phenylmethyl)amino]-

and 4-(Phenylamino)quinazolines as Potent Adenosine 5′-Triphosphate Binding Site Inhibitors of the Tyrosine Kinase Domain of the Epidermal Growth Factor Receptor. *J. Med. Chem.* **1995**, *38*, 3482−3487.

(11) Hennequin, L. F.; Thomas, A. P.; Johnstone, C.; Stokes, E. S. E.; Ple, P. A. et al. Design and Structure−Activity Relationship of a New Class of Potent VEGF Receptor Tyrosine Kinase Inhibitors. *J. Med. Chem.* **1999**, *42*, 5369−5389.

(12) Rewcastle, G. W.; Palmer, B. D.; Thompson, A. M.; Bridges, A. J.; Cody, D. R. et al. Tyrosine Kinase Inhibitors. 10. Isomeric 4-[(3-Bromophenyl)amino]pyrido[d]-pyrimidines Are Potent ATP Binding Site Inhibitors of the Tyrosine Kinase Function of the Epidermal Growth Factor Receptor. *J. Med. Chem.* **1996**, *39*, 1823−1835.

(13) Patil, S. A.; Otter, B. A.; Klein, R. S. Synthesis of Pyrrolo[2,1-*f*][1, 2, 4]triazine Congeners of Nucleic Acid Purines via the N−Amination of 2-Substituted Pyrroles [1]. *J. Heterocycl. Chem.* **1994**, *31*, 781−786.

(14) Fry, D. W.; Kraker, A. J.; McMichael, A.; Ambroso, L. A.; Nelson, J. M. et al. A Specific Inhibitor of the Epidermal Growth Factor Receptor Tyrosine Kinase. *Science* **1994**, *265*.

(15) Stamos, J.; Sliwkowski, M. X.; Eigenbrot, C. Structure of the Epidermal Growth Factor Receptor Kinase Domain Alone and in Complex with a 4-Anilinoquinazoline Inhibitor. *J. Biol. Chem.* **2002**, *277*, 46265−46272.

JM049892U